Appl. Magn. Reson. 21, 13–33 (2001)

Applied Magnetic Resonance

Zeeman Splitting Factor of the Er^{3+} Ion in a Crystal Field

C. A. J. Ammerlaan and I. de Maat-Gersdorf

Van der Waals-Zeeman Institute, University of Amsterdam, Amsterdam, The Netherlands

Received February 19, 2001

Abstract. Numerical computations are presented on the energy levels of the Er^{3+} ion in crystalline fields of cubic, trigonal, tetragonal and orthorhombic symmetry. Zeeman splitting factors were obtained from the level splitting in an additional magnetic field. For the quartet Γ_8 states in cubic symmetry the Zeeman effect is described by an effective Hamiltonian $\mathcal{H} = g\mu_B BJ + u\mu_B BJ^3$ with the parameters g and u calculated for mixed fourth- and sixth-order potentials. For the eight doublets in the lower symmetry of an axial trigonal or tetragonal crystal field the principal g tensor components $g_\parallel$ and $g_\perp$ were calculated. The results of such calculations for a ground-state doublet can exactly account for the experimental data obtained on around 70 erbium centers in various crystalline hosts. However, sometimes different sets of parameters give comparably good results. An empirical rule of constant trace $g_\parallel + 2g_\perp$ is supported by the calculations. In contrast to analytical treatments the effect of the crystalline field can be followed over a continuous range of the crystal field parameters. This allows one to establish relations on the relative signs of tensor components. It is found that the measured trace of tensors $|g_\parallel| + 2|g_\perp|$ is not always equal to their real trace $g_\parallel + 2g_\perp$. In an exploratory calculation a nonaxial center was simulated in an orthorhombic field, with calculation of the three principal values g_x, g_y and g_z. A good agreement is obtained for the recently reported g values of an erbium center in silicon.

1 Introduction

Magnetic resonance has provided valuable knowledge on the atomic and electronic structure of rare-earth impurities in crystalline hosts, such as in elemental and compound semiconductors. The spectroscopic information obtained by recording the angular dependence on magnetic field direction is commonly analyzed in the spin-Hamiltonian formalism. In the Hamiltonian as typically required, $\mathcal{H} = \mu_B BgJ + JAI$, the first term represents the Zeeman energy of the spin J in the magnetic field B, whereas the second term gives the hyperfine interaction energy with isotopes of nuclear spin I. By analyzing the experimental data the Zeeman splitting or g tensor and the hyperfine interaction tensor A, which commonly serve as a unique characterization of the spectrum, are determined. For the case of erbium, the isotope ^{167}Er has the nonzero spin $I = 7/2$ and is present with the natural abundance of 23%. For erbium, therefore, the structure of eight hyperfine satellite lines, to first order symmetrically displaced with respect to the central line of the $I = 0$ isotopes and with an intensity of 3.7% of the central line, is expected. Observation

Table 1. Principal g values of Er^{3+} spectra in various semiconductor and insulator host crystals.

Host	Symmetry	Principal g values		Trace of **g**	Reference(s)
Isotropic		g			
GaAs	cubic	5.92		17.76	48, 52, 53, 58
ZnS	cubic	5.926		17.778	26, 33, 50
ZnSe	cubic	5.950		17.850	30, 33, 50, 54
ZnSe	cubic	5.925		17.775	26
ZnTe	cubic	5.931		17.793	26, 33, 36, 50
CdTe	cubic	5.941		17.823	26, 33, 36, 50
CaF_2	cubic	6.785		20.355	6–8, 14, 16, 20, 22, 25, 28, 41, 42,
SrF_2	cubic	6.775		20.325	35, 42
SrF_2	cubic	6.803		20.409	27
BaF_2	cubic	6.755		20.265	27
CdF_2	cubic	6.76		20.28	12, 17
ThO_2	cubic	6.752		20.256	18, 20
CeO_2	cubic	6.759		20.277	20
Axial		$g_{\parallel}$	$g_{\perp}$		
Si	≈trigonal	0.45	≈3.34	7.13	1
Si	trigonal	0.69	3.24	7.17	1, 2
Si	trigonal	2.00	6.23	14.46	1, 2
InP	axial	5.699	5.954	17.607	49, 53
ZnS	axial	12.33	2.81	17.95	33, 50
ZnS	axial	2.423	8.771	19.965	33, 50
ZnTe	trigonal	1.245	9.469	20.183	36, 50
ZnTe	trigonal	4.066	8.068	20.202	36, 50
CdS	axial	11.415	1.675	14.765	33, 50
CdS	axial	3.240	8.019	19.278	33, 50
CdTe	trigonal	4.301	7.919	20.139	36
MgO	tetragonal	12.4	0.5	13.4	15
CaO	tetragonal	4.730	7.86	20.45	13
CaF_2	trigonal	3.672	8.27	20.212	47
CaF_2	trigonal	3.30	8.54	20.38	14, 25, 28, 41, 42, 51
CaF_2	trigonal	2.206	8.843	19.892	14, 16
CaF_2	trigonal	2.185	8.828	19.841	22, 28, 42
CaF_2	trigonal	2.183	9.015	20.213	17
CaF_2	trigonal	6.31	2.14	10.59	16, 28
CaF_2	trigonal	10.29	1.475	13.24	28, 42
CaF_2	trigonal	10.77	1.561	13.892	42
CaF_2	tetragonal	7.78	6.254	20.288	6–8, 14, 16, 22, 25, 28, 41, 42, 47
CaF_2	tetragonal	7.465	6.1	19.665	47
CaF_2	tetragonal	1.746	9.16	20.066	14, 28, 47
SrF_2	trigonal	6.179	7.054	20.287	27, 35, 42
SrF_2	trigonal	2.147	8.91	19.967	42
SrF_2	tetragonal	10.04	4.632	19.304	35, 42
BaF_2	trigonal	5.94	7.13	20.20	27
BaF_2	tetragonal	5.908	7.411	20.730	17
ThO_2	tetragonal	3.462	7.624	18.710	18
$LaCl_3$	trigonal	1.989	8.757	19.503	5, 7, 24

Table 1 (continued).

Host	Symmetry	Principal g values			Trace of **g**	Reference(s)
$LiYF_4$	tetragonal	3.137		8.105	19.347	40, 44, 46
$KMgF_3$	trigonal	4.216		7.886	19.988	39, 45
$KMgF_3$	trigonal	4.394		7.08	18.554	39
$KMgF_3$	tetragonal	2.682		8.362	19.406	39
$KZnF_3$	trigonal	4.390		7.813	20.016	43
$CaWO_4$	tetragonal	1.251		8.401	18.053	10, 21, 31, 32, 34, 38, 40
$SrWO_4$	tetragonal	0.86		8.47	17.80	38
$BaWO_4$	tetragonal	1.164		8.62	18.404	37, 38, 40
$CaMoO_4$	tetragonal	1.176		8.55	18.276	34, 38
$SrMoO_4$	tetragonal	1.019		8.43	17.879	29, 34, 37, 38
$PbMoO_4$	tetragonal	1.195		8.45	18.095	19, 34, 38, 40
$LiNbO_3$	trigonal	15.13		2.14	19.41	55
$La_{2-x}Sr_xCuO_4$	≈axial	1.3		9.3	19.9	H. Shimizi, pers. commun.
YES[a]	trigonal	1.50		8.77	19.04	23
LaES[b]	trigonal	1.47		8.85	19.17	3, 4, 23
Nonaxial		g_1	g_2	g_3		
Si	monoclinic-I	0.80	5.45	12.60	18.85	1, 56, 57
Si	monoclinic-I	0.80	5.45	12.55	18.80	1, 2, 56
Si	monoclinic-I	1.09	5.05	12.78	18.92	1, 2
Si	monoclinic-I	1.36	9.65	7.91	18.92	1
GaAs	orthorhombic	0.8	0.8	15.4	17.0	58
GaAs	orthorhombic	2.8	2.8	16.4	22.0	58
ZnSe	≈trigonal	0.57	8.877	12.032	21.479	54
$Lu_3Ga_5O_{12}$	orthorhombic	3.183	3.183	12.62	18.986	11
$Y_3Ga_5O_{12}$	orthorhombic	4.69	4.03	10.73	19.45	9, 11
$Lu_3Al_5O_{12}$	orthorhombic	6.93	4.12	8.43	19.48	11
$Y_3Al_5O_{12}$	orthorhombic	7.75	3.71	7.35	18.81	9, 11

[a] YES: $Y(C_2H_5SO_4)_3 \cdot 9H_2O$.
[b] LaES: $La(C_2H_5SO_4)_3 \cdot 9H_2O$.

of such hyperfine structure in the electron paramagnetic resonance (EPR) spectrum allows unambiguous identification of the erbium impurity. Unfortunately, due to the low abundance of the isotope the weak hyperfine lines are not always observable. For instance, this has been the case for recently described erbium centers in silicon [1, 2]. In this case the identification in magnetic resonance must rely on the fine structure tensor g of the Zeeman splitting. In order to assess the effect of a magnetic field on the paramagnetic rare-earth ion its electronic state as created by the stronger fields, i.e., firstly the spin-orbit interaction and secondly the crystal field, must be well known. The subject of this paper is the derivation of the g tensor of erbium centers in crystal fields of various symmetries. Energies of states are calculated with and without a magnetic field applied. Due to the high value of the electron spin and the complexity of the interactions, exact analytical solutions are restricted to some special cases only. Therefore, the calculations were carried out fully numeri-

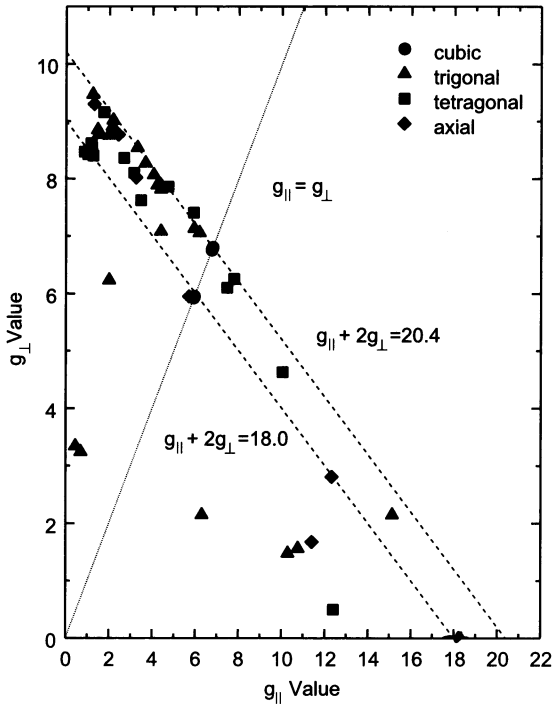

Fig. 1. Plot of values $g_{\perp}$ versus $g_{||}$ for magnetic resonance spectra of axial and isotropic Er^{3+} centers in several crystalline hosts corresponding to the data as given in Table 1. Dashed lines represent tensors with traces $g_{||} + 2g_{\perp} = 18.0$ and 20.4; in the isotropic case $g_{||} = g_{\perp} = 6$ for Γ_7 states and $g_{||} = g_{\perp} = 6.8$ for Γ_6 states.

cally. Reference is made to analytical solutions based on exact treatment or approximate perturbation methods when available. Over the last 40 years the EPR spectrum of the erbium ion as an impurity in several crystals, either in isolated form or as part of a complex, has been reported [1–58]. In the experiments the energy difference between Zeeman levels is measured and the g value is calculated as a positive number from the resonance condition $h\nu = g\mu_B B$, with $h\nu$ the microwave quantum. Only in an exceptional case the sign of g values was determined in a dedicated experimental setup [59]. Following this practice the principal spectroscopic parameters from experiment are given in Table 1 as positive. The g tensor data for isotropic and axial centers are as well represented in Fig. 1.

2 Method of Calculation

2.1 Spin-Orbit Interaction

For rare-earth ions the magnetic properties are dictated by the electrons in the incompletely filled 4f shell. For Er^{3+}, with the configuration $4f^{11}$, the orbital

momentum is $L = 6$ and the electron spin is $S = 3/2$. By the spin-orbit interaction λLS these states group into four levels with total angular momentum $J = L + S = 15/2$, $J = 13/2$, $J = 11/2$ and $J = L - S = 9/2$, respectively. As for the Er^{3+} ion the spin-orbit constant λ is negative, the state $J = 15/2$ forms the ground state. It is separated from the next higher state, with $J = 13/2$, by about 800 meV. Calculations are restricted to the isolated ground state with 16-fold degeneracy. In the spin J formalism the Landé factor for splitting in a magnetic field is $g_J = 1 + [J(J + 1) - L(L + 1) + S(S + 1)]/2J(J + 1) = 6/5$.

2.2 Crystal Field

Incorporated in a crystal the erbium ion is subject to the fields exerted by surrounding host atoms. In the crystal field the 16-fold degeneracy of the $J = 15/2$ spin-orbit level is lifted, the precise effect depending on strength and symmetry of the crystal field. For a high-symmetry cubic surrounding the splitting will be into three quartets and two doublets; for a low-symmetry field the maximum number of eight Kramers doublets will be obtained. Calculations of the energy levels were performed for centers of cubic, trigonal, tetragonal and orthorhombic symmetry. The crystal potentials are represented by their equivalent spin operators $\mathscr{H}_{cf}$. Crystal-field-induced splittings are of order of magnitude of 50 meV.

2.3 Magnetic Field

The Zeeman splitting of about 0.1 meV induced in an EPR experiment in the K-band (frequency, 23 GHz) is only a small perturbation on the states formed after spin-orbit and crystal-field interactions. Energies of the $J = 15/2$ spin-orbit ground state sublevels are calculated in the simultaneous presence of a crystal field and a magnetic field. The energy of the Zeeman effect is calculated by applying the operator $\mathscr{H}_{mf} = g_J \mu_B BJ$. By the magnetic field the degeneracy in the crystal-field quartet and doublet levels is lifted. By taking $\mu_B = 1$ and a magnetic field of unit strength, $|B| = 1$, the effective g values are directly obtained as the energy differences between levels. For example, in case of low symmetry $g_i = E_{i+} - E_{i-}$, $i = 1, \ldots, 8$. Calculations are restricted to the low-field regime with linear Zeeman splitting and consequently constant g values by proper scaling of the crystal-field coefficient. To match existing experimental conditions in the total spin Hamiltonian $\mathscr{H} = \mathscr{H}_{cf} + \mathscr{H}_{mf}$ the proportionality coefficient V_{cf} included in the expression for $\mathscr{H}_{cf}$ was usually given a value $V_{cf} = 1000$. The variation of this parameter V_{cf} over a wide range did have no effect on calculated g values. However, the computational scheme, in which only energies of states are calculated, is of a general nature and allows larger fields to be applied and nonlinear effects to be calculated without modification. Calculations have included centers from high cubic symmetry with isotropic EPR spectra and scalar g values, centers of trigonal and tetragonal symmetry with axial tensors

with principal values $g_{\|}$ and $g_{\perp}$, and centers of the lower orthorhombic or monoclinic symmetry with three independent principal g values, g_1, g_2 and g_3.

3 Cubic Symmetry

3.1 Energy

In case of cubic symmetry and f electrons the relevant crystal-field operators are of fourth and sixth order in spin J. The fourth-order operator is specified by

$$\mathscr{H}_{\mathrm{cu}4} = +O_4^0 + 5O_4^4 \tag{1a}$$

with

$$O_4^0 = +35J_z^4 - [30J(J+1) - 25]J_z^2 - 6J(J+1) + 3J^2(J+1)^2 \tag{1b}$$

and

$$O_4^4 = +(1/2)(J_+^4 + J_-^4)\,. \tag{1c}$$

The operator of sixth order is given by

$$\mathscr{H}_{\mathrm{cu}6} = +O_6^0 - 21O_6^4\,, \tag{2a}$$

with

$$O_6^0 = +231J_z^6 - 105[3J(J+1) - 7]J_z^4 + [105J^2(J+1)^2 - 525J(J+1) + 294]J_z^2 - 5J^3(J+1)^3 + 40J^2(J+1)^2 - 60J(J+1) \tag{2b}$$

and

$$O_6^4 = +(1/4)[11J_z^2 - J(J+1) - 38](J_+^4 + J_-^4) + (1/4)(J_+^4 + J_-^4)[11J_z^2 - J(J+1) - 38]\,. \tag{2c}$$

The linear combination

$$\mathscr{H}_{\mathrm{cf}} = V_{\mathrm{cf}}\mathscr{H}_{\mathrm{cu}} \tag{3a}$$

with

$$\mathscr{H}_{\mathrm{cu}} = \sin\alpha\mathscr{H}_{\mathrm{cu}4}/F_4 + \cos\alpha\mathscr{H}_{\mathrm{cu}6}/F_6 \tag{3b}$$

involving the two parameters V_{cf} and α, with α in the range of $-90° \le \alpha \le +90°$, represents the general case. To obtain more convenient values of parameters it is customary to introduce the dividers $F_4 = 60$ and $F_6 = 13860$ in Eq. (3b) [60–62]. Energy eigenvalues E of the Hamiltonian Eqs. (3) for $V_{\mathrm{cf}} = +1$ in the basis set of 16 states $m_J = -15/2$ to $+15/2$ are given in Fig. 2. For the doublet Γ_7 the exact result is $E = V_{\mathrm{cf}}(-40\cos\alpha + 294\sin\alpha)$, for the Γ_6 doublet $E = V_{\mathrm{cf}}(-312\cos\alpha - 26\sin\alpha)$. Energies of the quartet states $(\Gamma_8)_i$, $i = 1$, 2 and 3, are the numerically computed solutions of a cubic equation for each α. Except

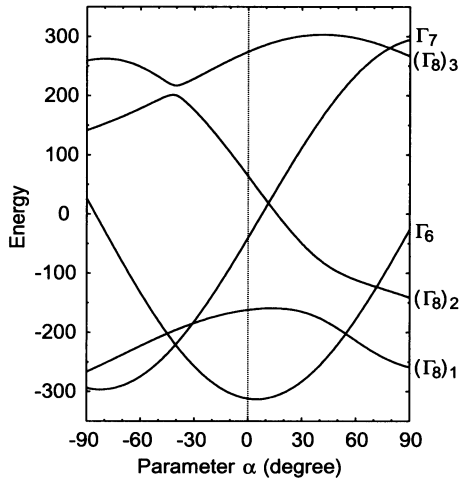

Fig. 2. Crystal-field energies of doublets Γ_6 and Γ_7 and of quartets $(\Gamma_8)_i$, $i = 1$, 2 and 3, in the cubic case representing the eigenvalues of Eqs. (3) with $V_{cf} = +1$. Parameter α in the range of $-90° \leq \alpha \leq 90°$ controls the mixing of the fourth- and sixth-order cubic crystal fields.

for the different choice of parameters the result is identical to the classical data of Lea et al. [61]. The two parameter sets are related by $V_{cf}\sin\alpha = Wx$ and $V_{cf}\cos\alpha = W(1 - |x|)$. Also, in accordance with more recent literature, the labels Γ_6 and Γ_7 have been interchanged. On the basis of a point charge model a positive value of V_{cf} is expected. If so, inspection of Fig. 2 shows that the ground state will be of doublet Γ_7 character for $-90° \leq \alpha \leq -40.4°$, of character Γ_6 for $-40.4° \leq \alpha \leq +54.5°$ and Γ_8 for $+54.5° \leq \alpha \leq +90°$. For a substitutional site of erbium, with a fourfold coordination of ligands, parameter α will be negative and the ground state will be the Γ_6 or Γ_7 doublet. On an interstitial site, with octahedrally coordinated neighbors and positive α, ground states of Γ_6 or Γ_8 character are possible.

3.2 g Value

Splitting of the doublet states in a magnetic field can be described by an effective spin $J = 1/2$ and labelling of the states as $|\pm\rangle$. In the cubic field the conjugate wave functions of the doublets are expressed in the basis states $|m_J\rangle$ of the $J = 15/2$ level by $\sum_J c_J|m_J\rangle$. For Γ_6 one obtains, independent of parameter α,

$$\begin{aligned}\left|\Gamma_{6\pm}\right\rangle = &+(1/24)\sqrt{231}\left|\pm 13/2\right\rangle + (1/24)\sqrt{195}\left|\pm 5/2\right\rangle \\ &-(1/8)\sqrt{13}\left|\mp 3/2\right\rangle - (1/24)\sqrt{33}\left|\mp 11/2\right\rangle . \end{aligned} \tag{4}$$

The splitting is isotropic with the effective g factor given by $g = 2g_J\sum_J c_J^2 m_J = 34/5$. In an equivalent way for Γ_7 the wave functions are

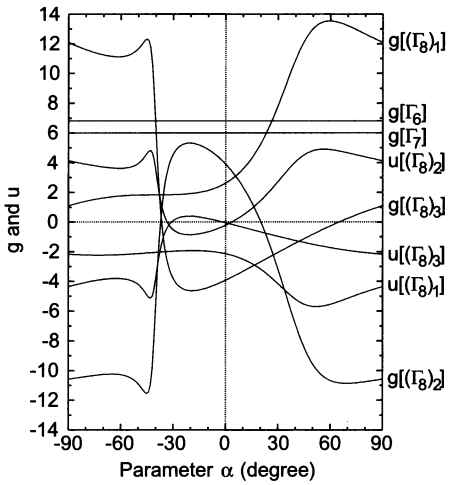

Fig. 3. g values of doublet and quartet levels in cubic symmetry pertaining to the Hamiltonian given in Eq. (6). Parameter α in the range of $-90° \leq \alpha \leq 90°$ controls the mixing of the fourth- and sixth-order contributions.

$$\begin{aligned}\left|\Gamma_{7\pm}\right\rangle = &+(1/24)\sqrt{195}\left|\pm 15/2\right\rangle + (1/8)\sqrt{7}\left|\pm 7/2\right\rangle \\ &+(1/8)\sqrt{33}\left|\mp 1/2\right\rangle + (1/24)\sqrt{21}\left|\mp 9/2\right\rangle\end{aligned} \tag{5}$$

and the isotropic effective g value is $g = 6$. From the values listed in Table 1 for the semiconductors GaAs, ZnS, ZnSe, ZnTe and CdTe the experimental values close to 6 indicate a Γ_7 ground state and the negative value of α confirms a substitutional erbium position. In contrast, for erbium in CaF_2, SrF_2, BaF_2, CdF_2, ThO_2 and CeO_2 a Γ_6 ground state is indicated by the g value. The small negative deviations of experimental values from the calculated numbers are discussed in several papers and have been ascribed to admixture of the higher terms $^2K_{15/2}$ and $^2L_{15/2}$, admixture of Γ_8 state by the magnetic field and covalent delocalization [13, 26, 30, 48, 63]. It may be concluded that the theoretical description provides good agreement with experimental data. However, a precise value of parameter α cannot be derived. For quartet states Γ_8 the splitting of the four levels in a magnetic field can be described by effective spin $J = 3/2$ and the cubic spin Hamiltonian

$$\mathscr{H} = g\mu_B BJ + u\mu_B(B_x J_x^3 + B_y J_y^3 + B_z J_z^3). \tag{6}$$

Numerically calculated values for g and u for the three quartet levels are given in Fig. 3. It can be observed that in the crystal field the coefficient u of the cubic operator is not always small compared to the g value of the magnetic-dipole Zeeman effect. For this reason the angular dependence of the anisotropic resonance must be described by the general expression

$$g_{\pm} = +\{+5g^2 + 41gu/2 + 365u^2/16 \pm [+(+16g^4 + 160g^3u + 582g^2u^2 + 910gu^3 + 8281u^4/16) - (+144g^3u + 864g^2u^2 + 1701gu^3 + 2205u^4/2)\sin^2\theta + (+108g^3u + 648g^2u^2 + 5103gu^3/4 + 6615u^4/8)\sin^4\theta]^{1/2}\}^{1/2} . \quad (7)$$

The result applies to the usual measurement in which the magnetic field is rotated in an (011) plane with the angle θ to the [100] direction. Signs $\pm$ refer to the outer and inner doublets of the quartet system. The approximation valid for $u \ll g$, leading to the familiar angular dependence following the function $p(\theta) = 1 - 5\sin^2\theta + (15/4)\sin^4\theta$, breaks down [30, 62, 64, 65].

4 Trigonal and Tetragonal Symmetry

4.1 Energy

As can be noted in Table 1, several erbium-related centers were found to have axial symmetry. Their symmetry was either established as trigonal, with axis along a $\langle 111 \rangle$ direction, tetragonal, with axis along $\langle 100 \rangle$, or the axis was left unspecified. In the trigonal case the leading crystal-field operator of second order is given by

$$\mathscr{H}_{\mathrm{tr}} = -(1/4)\,\mathrm{i}J_+^2 + (1/4)\,\mathrm{i}J_-^2 + (1/4)(1-\mathrm{i})J_+J_z + (1/4)(1-\mathrm{i})J_zJ_+ + (1/4)(1+\mathrm{i})J_-J_z + (1/4)(1+\mathrm{i})J_zJ_- \quad (8)$$

in the Cartesian coordinate system. Including a cubic contribution as well, the general crystal-field operator will be expressed by

$$\mathscr{H}_{\mathrm{cf}} = V_{\mathrm{cf}}\mathscr{H}_{\mathrm{cu\,tr}} \quad (9a)$$

with

$$\mathscr{H}_{\mathrm{cu\,tr}} = \cos\beta\mathscr{H}_{\mathrm{cu}} + \sin\beta\mathscr{H}_{\mathrm{tr}}/F_2 \quad (9b)$$

and with parameter β, in the range of $-90° \le \beta \le +90°$, specifying the cubic and trigonal components. A factor $F_2 = 0.1$ is included in the trigonal field term to obtain better match of the two contributions in the $J = 15/2$ spin system. In the trigonal field all orbital degeneracy is removed and the spectrum will consist of eight doublet levels. For two selected cases of parameter α, $\alpha = -90°$ and $\alpha = +30°$, the energy eigenvalues of $\mathscr{H}_{\mathrm{cu\,tr}}$ are shown in Fig. 4a and b. Treating the case of the tetragonal field in a similar way, the pertinent second-order crystal-field operator is

$$\mathscr{H}_{\mathrm{te}} = +J_z^2 - (1/3)J(J+1) . \quad (10)$$

Combined with a cubic field the total crystal-field operator will be

$$\mathscr{H}_{\mathrm{cf}} = V_{\mathrm{cf}} \mathscr{H}_{\mathrm{cu\,te}}\,, \tag{11a}$$

with

$$\mathscr{H}_{\mathrm{cu\,te}} = \cos\beta \mathscr{H}_{\mathrm{cu}} + \sin\beta \mathscr{H}_{\mathrm{te}} / F_2\,, \tag{11b}$$

again with $-90° \leq \beta \leq +90°$. Energies of eight doublets as a function of β computed with $V_{\mathrm{cf}} = +1$ for two values of α, $\alpha = -90°$ and $\alpha = +30°$, are given in

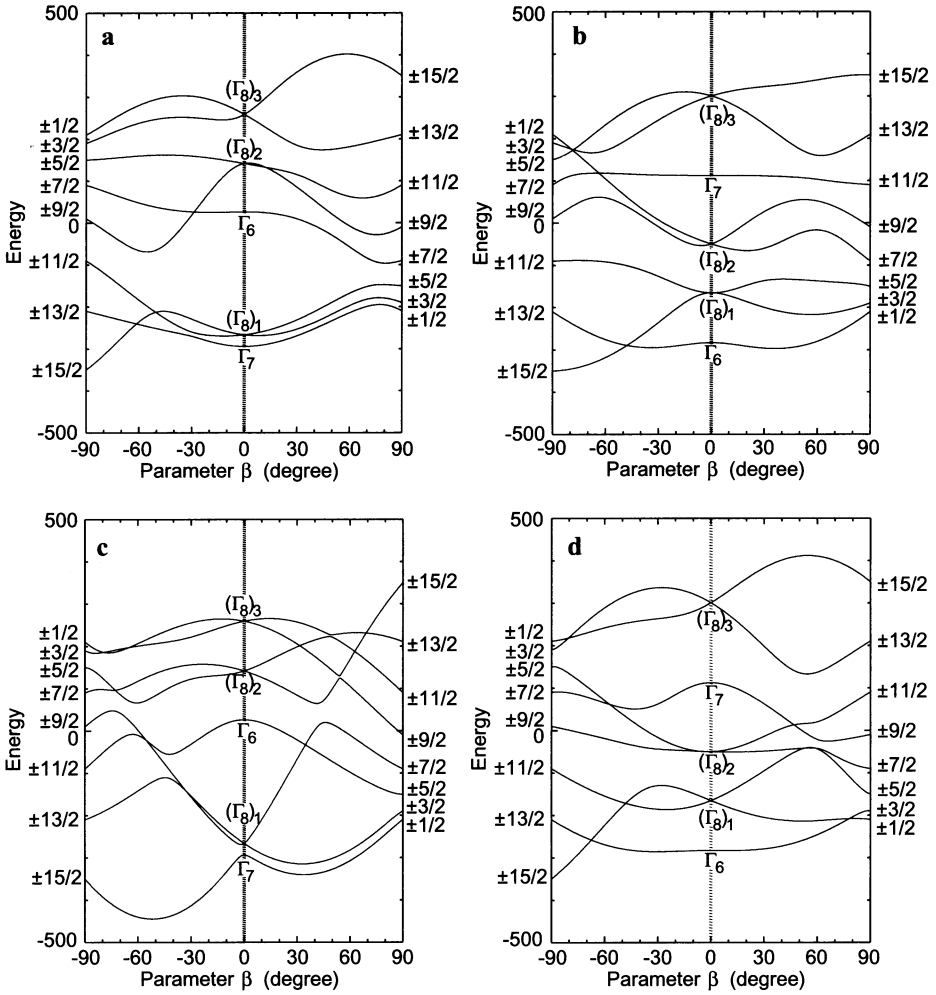

Fig. 4. Energies of eight doublets for fourth- or sixth-order cubic crystal field together with a second-order trigonal or tetragonal crystal field, calculated from Eqs. (9) or (10) with $V_{\mathrm{cf}} = +1$ for **a** $\alpha = -90°$, trigonal; **b** $\alpha = +30°$, trigonal; **c** $\alpha = -90°$, tetragonal; **d** $\alpha = +30°$, tetragonal. Parameter β in the range of $-90° \leq \beta \leq +90°$ controls the mixing of the cubic and axial crystal fields.

Fig. 4c and d. For the limiting values $\beta = \pm 90°$ only the axial trigonal or tetragonal field is present. In this field the states quantize as $|15/2, \pm m_J\rangle$, with the quantization axis taken along the axial direction. The corresponding energies of $\mathscr{H}_{\mathrm{cu\,tr}}$ and $\mathscr{H}_{\mathrm{cu\,te}}$ are ± 210, ± 190, ± 150, ± 90, ± 10, ∓ 90, ∓ 210 and ∓ 350, in a way as can be verified in Fig. 4. For $V_{\mathrm{cf}} = +1$, as used to draw Fig. 4, the lowest level forms the ground state in which magnetic resonance is observed. For negative V_{cf} the roles of highest and lowest level interchange. Inspection of Figs. 2 and 4 reveals that the ground state can have Γ_6, Γ_7 or Γ_8 symmetry type in cubic field, and be of $m_J = \pm 1/2$ or $\pm 15/2$ character in the pure axial situation. It might be remarked here that among states $|15/2, \pm m_J\rangle$ only the doublet $|15/2, \pm 1/2\rangle$ will give an observable magnetic resonance transition. All other doublets have $g_\perp = 0$, preventing the observation of spin resonance.

4.2 g Value

Splitting of the spin doublet levels in a magnetic field is expressed by their Zeeman splitting or g factors. Effective g values for the parallel and perpendicular directions in trigonal and tetragonal symmetry were computed by diagonalization of the 16×16 matrices of the operator $\mathscr{H}_{\mathrm{cf}} + \mathscr{H}_{\mathrm{mf}}$ as a function of the parameters α and β. In the computations as actually carried out parameter β was varied in the range of -90 to $+90$ degrees in steps of 0.1 degree, for values of α spanning the same range in steps of 10 degrees. Reviewing the results and observing the complex behavior of g tensor variations one must conclude that a comprehensive and quantitatively accurate analytical treatment of Zeeman effects for a spin system $J = 15/2$ in crystal fields is beyond feasibility. To allow a direct comparison with experimental data as presented in Fig. 1, in Fig. 5 the calculated perpendicular g value $g_\perp$ is plotted as a function of the calculated parallel value $g_\parallel$ for the same β. In an additional presentation of results, Fig. 6 shows the $g_\parallel$ and $g_\perp$ values in their dependence on parameter β. In Figs. 4–6 the panels a correspond to trigonal centers with $\alpha = -90°$, b trigonal, $\alpha = +30°$, c tetragonal, $\alpha = -90°$, and d tetragonal, $\alpha = +30°$, selected for optimal illustration of the vast amount of data points and the systematics in their behavior. In cases a and c, for $\beta = 0$ the ground state is Γ_7 and the isotropic g value $g = 6$ is reproduced. For cases b and d the ground state is Γ_6 with $g = 6.8$. It was shown by Lewis and Sabisky [63] that for small axial perturbations the trace $g_\parallel + 2g_\perp$ of the g tensors will stay constant. Inspection of Figs. 5 or 6 shows that the theoretical result is unambiguously confirmed for both Γ_6 and Γ_7 doublets, both upon trigonal or tetragonal distortion with small β, and irrespective of parameter α characterizing the cubic field. Not shown in the figures, the rule holds equally well if the levels do not form the ground state. Considering next the range of large axial distortions, for $\beta = +90°$ and $V_{\mathrm{cf}} > 0$ the ground state in the purely axial field is $|15/2, m_J = \pm 1/2\rangle$. Exact g values for this state are derived as $g_\parallel = 1.2$ and $|g_\perp| = 9.6$. From Fig. 6b for $\alpha = +30°$ it is concluded that $g_\parallel$ and $g_\perp$ have

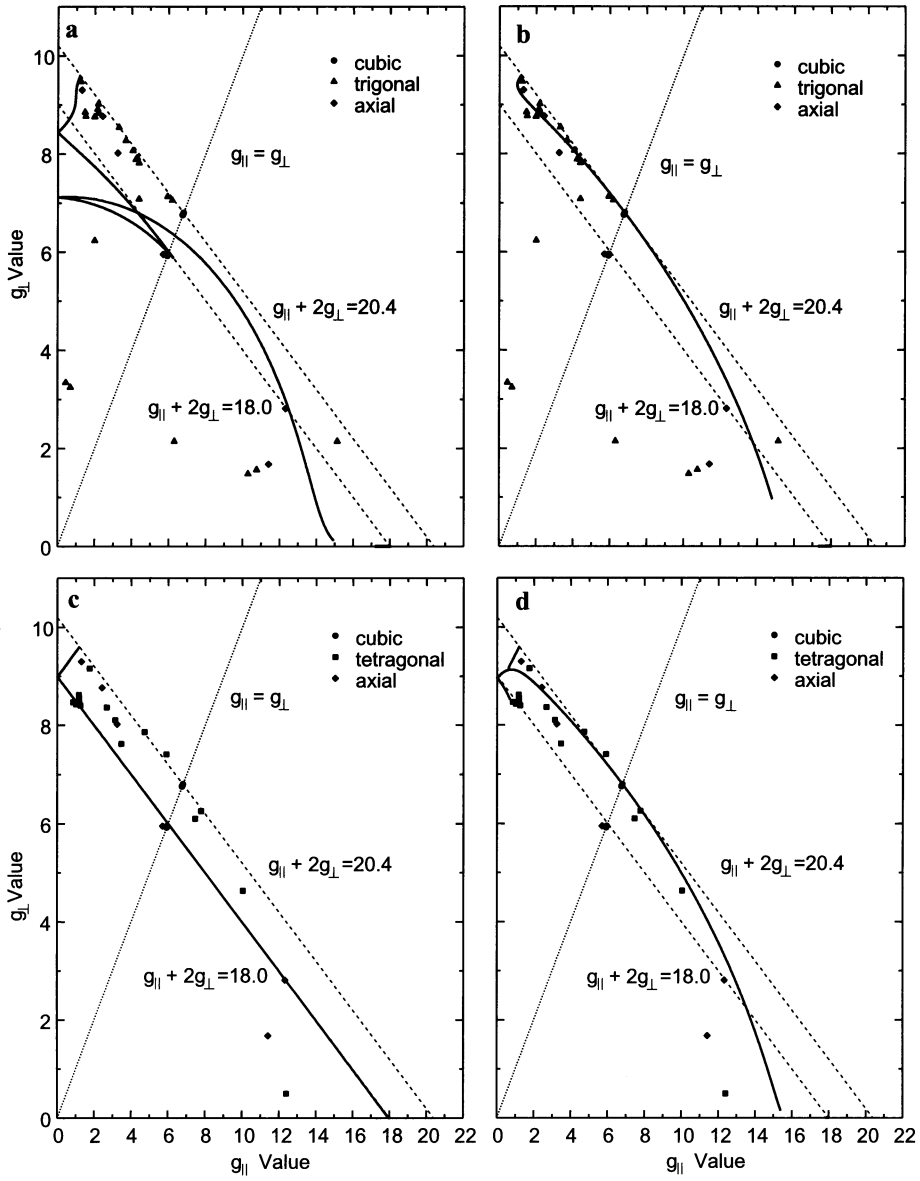

Fig. 5. Plot of $g_{\perp}$ versus $g_{||}$ calculated for lowest-energy doublets for **a** $\alpha = -90°$, trigonal; **b** $\alpha = +30°$, trigonal; **c** $\alpha = -90°$, tetragonal; **d** $\alpha = +30°$, tetragonal.

the same sign, hence at $\beta = +90°$ the trace $g_{||} + 2g_{\perp} = 20.4$, equal to the trace at the isotropic point $\beta = 0°$. For $\alpha = -90°$, Fig. 6a shows $g_{||}$ to change sign in the range from $\beta = 0°$ to $\beta = +90°$, at around $\beta = +47°$. Assuming $g_{||} = +1.2$ at $\beta = +90°$, equal to the Landé factor $g = 6/5$, it must be concluded that $g_{\perp}$ at $\beta = +90°$ has the negative value of -9.6. As the sign escapes de-

tection, the measured trace $|g_{\|}| + 2|g_{\perp}| = 20.4$ would easily lead to the erroneous conclusion that the state is Γ_6 related. At $\beta = 0°$, for the Γ_7 state in cubic symmetry, the g value must be -6, but, again, as the sign is not determined in the standard experiment, the commonly reported value is positive. The corresponding traces are equal at both β points at -18. Also for tetragonal sym-

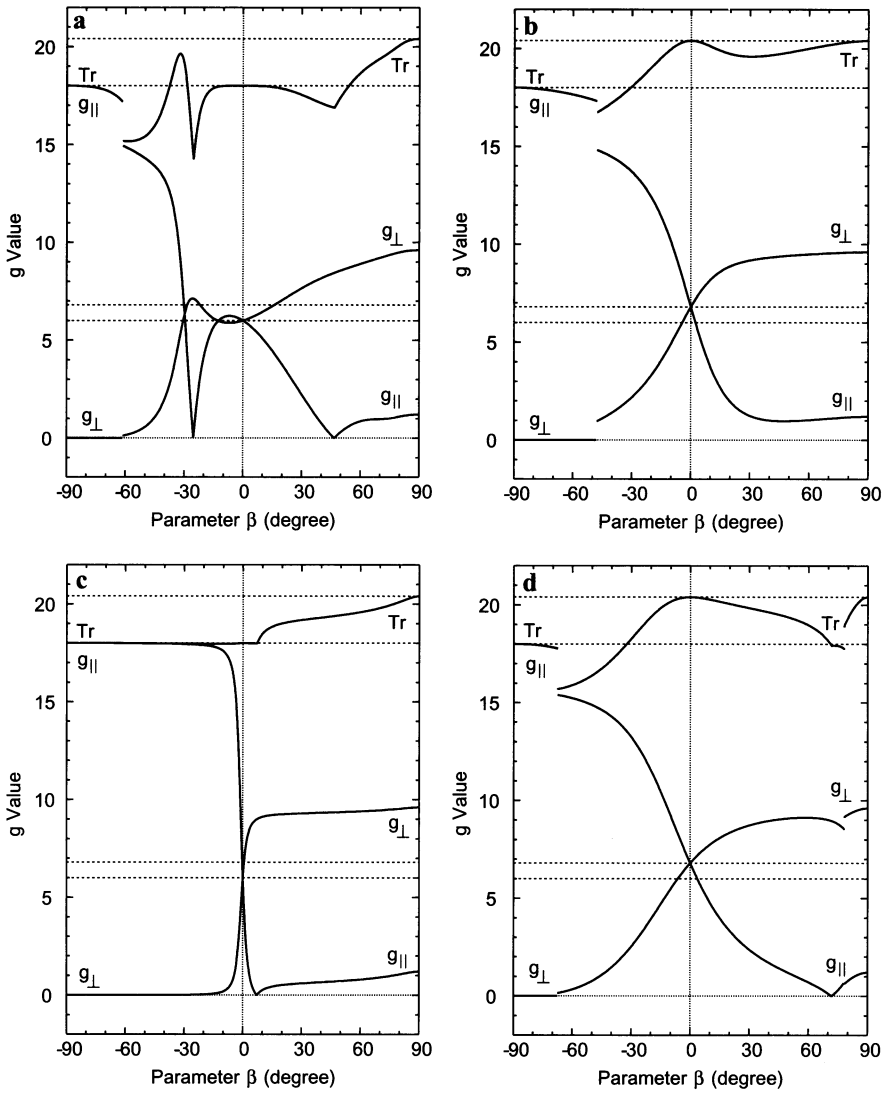

Fig. 6. g Values of lowest-energy doublet states including $g_{\|}$, $g_{\perp}$ and trace $g_{\|} + 2g_{\perp}$ as a function of parameter β for **a** $\alpha = -90°$, trigonal; **b** $\alpha = +30°$, trigonal; **c** $\alpha = -90°$, tetragonal; **d** $\alpha = +30°$, tetragonal. Parameter β in the range of $-90° \leq \beta \leq +90°$ controls the mixing of the cubic and axial crystal fields.

metry, as demonstrated by Figs. 5c, d, and 6c, d, the trace at $\beta = +90°$ is exactly equal to its value at $\beta = 0°$. In the region in between a reduction is calculated, but in several cases the trace remains remarkably constant. This is especially true for the case illustrated by Figs. 5c and 6c. For this lowest level in tetragonal symmetry and fourth-order cubic field, $\alpha = -90°$, the trace in the whole range for β never falls more than 0.3% below the value 18 for the Γ_7 state. In no case a calculated trace exceeds the value 20.4. The great majority of the experimental tensors, shown in Fig. 1 in the upper left part, have their trace values slightly below the line $g_{\|} + 2g_{\perp} = 20.4$. These data are well fitted by the computed curves as shown in Figs. 5b and 6b for trigonal and Figs. 5d or 6d for tetragonal centers. It can be concluded that the calculations can well account for the observed g values, thus confirming that they are properly interpreted as due to the $J = 15/2$ spin system of erbium ions. In the results as illustrated in Figs. 5 and 6 agreement is reached for $\alpha = +30°$ and β values near $+20°$. It must, however, be emphasized that very similar calculated results and consequently similar agreement is achieved for parameter α in the range of -30 to $+50°$, in which the Γ_6 level is ground state in cubic symmetry. The data as given above for good agreement are therefore not unique. Just

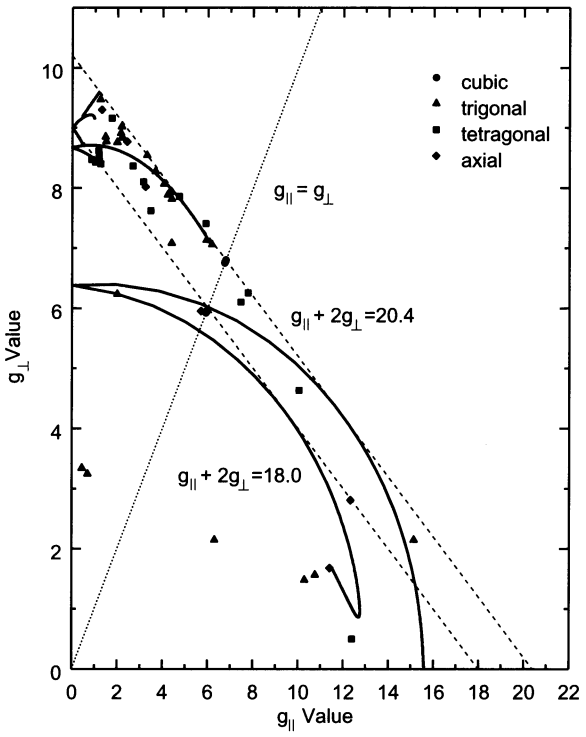

Fig. 7. Plot of $g_{\perp}$ versus $g_{\|}$ calculated for lowest-energy doublet in tetragonal symmetry for parameter $\alpha = +80°$.

as for the cubic centers, a precise value of α cannot be determined by the analysis. Good fits, though not as convincing and systematic, can also be found in completely different ranges of parameters, e.g., for negative value of V_{cf}. Unfortunately this ambiguity, related to the complexity of interactions, does not allow the above solutions to be presented as unique. In Fig. 1 also a few data points are included for which $g_{\|} > g_{\perp}$. An illustration of their matching by the crystal field calculation is given in Fig. 7, which shows the $g_{\|}$-versus-$g_{\perp}$ relation for the lowest level in tetragonal symmetry for $\alpha = +80°$. At the same time Fig. 7 shows alternative interpretations of the data points in the upper-left corner of the plot, underlining the necessity of care in conclusively selecting matching parameters. In summary, all experimental data points can be accounted for in the calculations, with the exception of the tensors OEr-2 and OEr-2′ for centers in silicon [1]. Their identification as erbium related is therefore not supported by the present analysis.

5 Orthorhombic Symmetry

5.1 Energy

To explore the spectroscopic properties of low-symmetry centers the case of an orthorhombic crystal field in addition to a tetragonal field was considered. In this restriction to $\beta = \pm 90°$ a cubic field was left outside consideration. The second-order operator corresponding to the orthorhombic field is written as

$$\mathcal{H}_{or} = +(1/6)\sqrt{3}(J_+^2 + J_-^2) \tag{12}$$

and is normalized with respect to the tetragonal operator $\mathcal{H}_{te}$. The general expression for the mixed tetragonal-orthorhombic field is

$$\mathcal{H}_{cf} = V_{cf}\mathcal{H}_{te\ or} \tag{13a}$$

with

$$\mathcal{H}_{te\ or} = \cos\gamma\mathcal{H}_{te} + \sin\gamma\mathcal{H}_{or}. \tag{13b}$$

Variation of parameter γ over the range of $0° \leq \gamma \leq +30°$ is sufficient to cover all basically different fields. Energies of the eight doublet states obtained from the diagonalization of Hamiltonian Eq. (13) are given in Fig. 8 as a function of parameter γ. It is noted that level crossings do not appear. For positive V_{cf}, the expected case, the level related to the state $|J = 15/2,\ m_J = \pm 1/2\rangle$ with the energy $E = -21$ at $\gamma = 0°$ will always be the ground state. In case of small non-axial distortion a perturbation treatment can be applied. It leads to the analytical expression

$$E = V_{cf}\cos\gamma[-21 - (441/2)\,\mathrm{tg}^2\gamma] \tag{14}$$

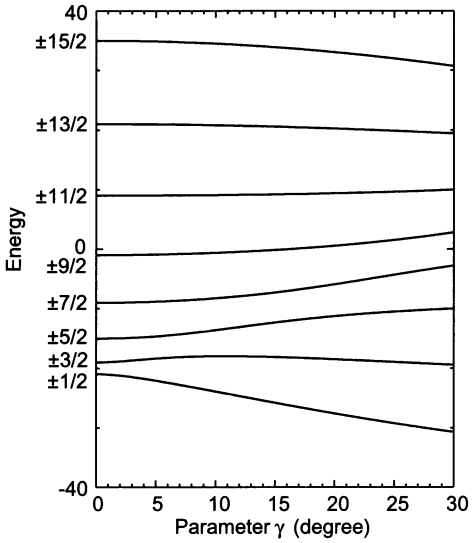

Fig. 8. Energies of eight doublets in tetragonal axial field together with an orthorhombic crystal field calculated from Eqs. (13) with $V_{cf} = +1$. Parameter γ in the range of $0° \leq \gamma \leq +30°$ controls the relative contributions of the two crystal fields.

for the energy of the lowest state. This is in good agreement with the numerically calculated curve but only up to about 3°. The wave function of the perturbed $|\pm 1/2\rangle$ state is found to be

$$|\pm 1/2\rangle' = |\pm 1/2\rangle - (1/2)\sqrt{35}\,\mathrm{tg}\,\gamma|\pm 5/2\rangle - 2\sqrt{21}tg\gamma|\pm 3/2\rangle \tag{15}$$

in a nonnormalized form. Similar expressions exist for the other m_J values.

5.2 g Value

As before, the Zeeman effect is treated by diagonalization of the matrix $\langle m'_J|\mathscr{H}_{cf} + \mathscr{H}_{mf}|m''_J\rangle$. Principal values of the g tensor in the Cartesian x, y, z directions are drawn in Fig. 9 for the level derived from $m_J = \pm 1/2$ in tetragonal axial symmetry. Experimental data points for the OEr-1 center observed in silicon are included in Fig. 9 [1]. A good agreement can be noted for $\gamma \approx 1.2°$, providing confirmation for the assumed relation of the spectrum with the $J = 15/2$ of erbium. With the wave function Eq. (15) for the ground state available, the Zeeman splitting can be calculated by treating it as a small perturbation. On this basis the expressions for the principal g tensor components are

$$g_x = +g_J(+6\sqrt{7}c_{3/2}c_{1/2} + 4\sqrt{15}c_{3/2}c_{5/2} + 8c_{1/2}^2)\,, \tag{16a}$$

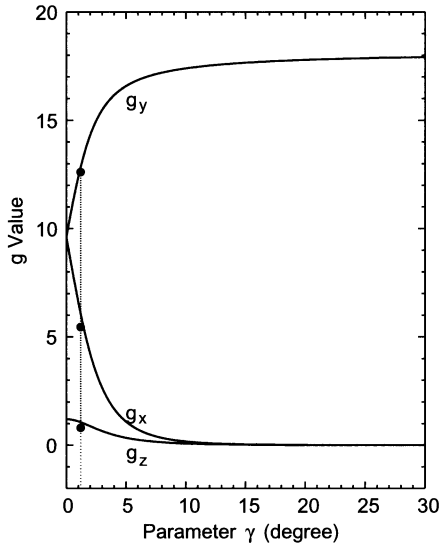

Fig. 9. Principal g values g_x, g_y and g_z for a center with orthorhombic symmetry as a function of parameter γ for the ground state level. Experimental data points are for the erbium center in silicon, spectrum Si-OEr-1 from Carey et al. [1].

$$g_y = +g_J(-6\sqrt{7}c_{3/2}c_{1/2} + 4\sqrt{15}c_{3/2}c_{5/2} + 8c_{1/2}^2)\,, \tag{16b}$$

$$g_z = +g_J(+3c_{3/2}^2 - c_{1/2}^2 - 5c_{5/2}^2)\,. \tag{16c}$$

Inserting the wavefunction coefficients as following from Eq. (15) after their normalization, and with $g_J = 6/5$, one obtains

$$g_x = +\frac{6}{5}\cdot\frac{8 - 84\sqrt{3}\,\mathrm{tg}\gamma + 420\,\mathrm{tg}^2\gamma}{1 + (371/4)\,\mathrm{tg}^2\gamma}\,, \tag{17a}$$

$$g_y = +\frac{6}{5}\cdot\frac{8 + 84\sqrt{3}\,\mathrm{tg}\gamma + 420\,\mathrm{tg}^2\gamma}{1 + (371/4)\,\mathrm{tg}^2\gamma}\,, \tag{17b}$$

$$g_z = +\frac{6}{5}\cdot\frac{1 - (833/4)\,\mathrm{tg}^2\gamma}{1 + (371/4)\,\mathrm{tg}^2\gamma}\,. \tag{17c}$$

It is seen from Fig. 9 that the most sensitive indication for the nonaxial distortion is given by the lifting of the $g_\perp$ degeneracy, i.e., by $g_y - g_x$. By Eqs. (17) this difference equals

$$g_y - g_x = +\frac{1008}{5}\cdot\frac{\sqrt{3}\,\mathrm{tg}\gamma}{1 + (371/4)\,\mathrm{tg}^2\gamma}\,. \tag{18}$$

With the experimental result for the Si-OEr-1 center $g_y - g_x = 7.15$, its γ parameter is determined as $\gamma = 1.2°$.

6 Conclusions

Calculations have been performed of the electronic structure of the triply charged erbium ion in its spin-orbit ground level with spin $J = 15/2$ when embedded as an impurity in a host crystal. Calculations were carried out fully numerically. Employing a crystal field method the energy levels and wave functions were determined for the ion in Stark fields of cubic, trigonal, tetragonal and orthorhombic symmetry, created by the ligand ions of the crystal. The relative contributions of the crystal fields of isotropic, axial and nonaxial symmetry are described by mixing parameters α, β and γ. Also the principal components of g tensors for the Zeeman splitting were calculated by applying a magnetic field in the appropriate directions. In previous theoretical determinations of g values, with analytical methods, exact results were restricted to the Γ_6 and Γ_7 states in pure cubic symmetry and the states $|J = 15/2, m_J\rangle$ in fields of pure axial character. In contrast, in the numerical calculations fields of arbitrary structure can be constructed as the parameters α, β and γ can be varied continuously over a range covering all situations. Considering calculated results it is noted that the parallel principal g value $g_{\|}$ in axial symmetry can change its sign upon variation of parameter β, governing the relative contributions of cubic and axial fields. Accepting a positive value for $g_{\|}$ in the purely axial situation of $\beta = +90°$, where the quantization of spin states is more straightforward, a negative value for g appears in the cubic situation. In particular, for the Γ_7 state of cubic symmetry the consistent g value is found as $g = -6$. In experiment the absolute value $g = 6$ will be measured. From collected experimental data, obtained for a large number of varied host crystals, the trace $|g_{\|}| + 2|g_{\perp}|$ of g tensors for the erbium-related resonances was found often to be close to 20.4, i.e., the trace of the cubic center in the Γ_6 state. An empirical rule of constant trace upon axial distortion with consequences for the electronic origin of the impurity states can be based on this observation. Such a rule has to be applied with care, however, as by taking signs into account the real trace can be different from the measured trace based on absolute positive values. For instance, in case of axial symmetry, a real trace of $g_{\|} + 2g_{\perp} = -18$, based on $g_{\|} = +1.2$ and $g_{\perp} = -9.6$ and derived from Γ_7, is measured as a trace of 20.4 and interpreted as having a Γ_6 origin. In rare cases only, negative g values have been concluded to for consistent analysis of experimental data, such as for the Yb ion in $KMgF_3$ [66]. Because of a complex dependence of g values on crystal field parameters α and β, with often wide and sudden variations, the comprehensive summary of results is hard to give. Nevertheless, it is noted that over a wide range of α values, controlling the mixing of fourth- and sixth-order cubic crystal fields, the trace of tensors remains remarkably constant upon a distortion with positive β towards the $|J = 15/2, m_J = \pm 1/2\rangle$ doublet. This accounts in an uncomplicated manner for the frequently observed tensors with

trace near 20.4. One may conclude that the crystal-field approach provides a valid description of the spin system. It is also to be noted that equal or very similar g values are calculated over a range of parameters. For the cubic centers, the g values $g = 6$ for Γ_7 and $g = 6.8$ for Γ_6 do not depend at all on parameter α. For the axial case, different combinations of parameters α and β can give results not distinguishable by the experiments. Parameters α and β are therefore not obtained from the analysis unambiguously or with great precision. Additional information is required for full characterization. Such data are provided by studies of the first excited state of the Stark splitting, such as the direct spectroscopic measurement of their Zeeman splitting, as reported, e.g., for the axial erbium center in CaF_2 [6, 47] and for tungstate and molybdate matrices [31, 34, 37, 38]. In addition, from the population of this level as a function of temperature the excitation energy can be derived via the associated Boltzmann factor [6]. Alternatively, the position of the first excited states has been determined from the ground state resonance through the Orbach process of spin-lattice relaxation [17, 23, 24, 28, 31, 38, 43, 67]. More direct and more complete data on the position of the five to eight crystal-field split levels can come from optical spectroscopy in the form of structure in the photoluminescence spectra, but this requires firm knowledge that the centers studied in both techniques are equal [22, 25, 29, 30, 47, 54, 55]. For the interpretation of results from optically detected magnetic resonance and from optical Zeeman measurements calculations of the same nature as presented in this paper have to be extended to include the $J = 13/2$ first optically excited state at around 800 meV. Other topics for future research include the thorough investigation of centers of quartet Γ_8 character in cubic symmetry and the systematic exploration of g tensors for low-symmetry centers in their α, β and γ field of parameters.

References

1. Carey J.D., Barklie R.C., Donegan J.F., Priolo F., Franzò G., Coffa S.: Phys. Rev. B **59**, 2773–2782 (1999)
2. Carey J.D., Priolo F.: Physica **273-274**, 350–353 (1999)
3. Elliott R.J., Stevens K.W.H.: Proc. R. Soc. Lond. A **219**, 387–404 (1953)
4. Bowers K.D., Owen J.: Rep. Prog. Phys. **18**, 304–373 (1955)
5. Hutchison C.A. Jr., Wong E.: J. Chem. Phys. **29**, 754–760 (1958)
6. Baker J.M., Hayes W., Jones D.A.: Proc. Phys. Soc. Lond. **73**, 942–945 (1959)
7. Orton J.W.: Rep. Prog. Phys. **22**, 204–240 (1959)
8. Dvir M., Low W.: Proc. Phys. Soc. Lond. **75**, 136–138 (1960)
9. Ball M., Garton G., Leask M.J.M., Ryan D., Wolf W.P.: J. Appl. Phys. **32**, 267S–269S (1961)
10. Mims W.B., Nassau K., McGee J.D.: Phys. Rev. **123**, 2059–2069 (1961)
11. Wolf W.P., Ball M., Hutchings M.T., Leask M.J.M., Wyatt A.F.G.: J. Phys. Soc. Jpn. **17**, Suppl. 2, 443–448 (1962)
12. Zverev G.M., Kornienko L.S., Prokhorov A.N., Smirnov A.I.: Sov. Phys. Solid State **4**, 284–286 (1962) [Fiz. Tverd. Tela **4**, 392–395 (1962)]
13. Low W., Rubins R.S.: Phys. Rev. **131**, 2527–2528 (1963)
14. Ranon U., Low W.: Phys. Rev. **132**, 1609–1611 (1963)
15. Descamps D., Merle d'Aubigne Y.: Phys. Lett. **8**, 5–7 (1964)
16. Weber M.J., Bierig R.W.: Phys. Rev. **134**, A1492–A1503 (1964)

17. Zverev G.M., Smirnov A.I.: Sov. Phys. Solid State **6**, 76–79 (1964) [Fiz. Tverd. Tela **6**, 96–100 (1964)]
18. Abraham M., Weeks R.A., Clark G.W., Finch C.B.: Phys. Rev. **137**, A138–A142 (1965)
19. Antipin A.A., Katyshev A.N., Kurkin I.N., Shekun L.Ya.: Sov. Phys. Solid State **7**, 1148–1149 (1965) [Fiz. Tverd. Tela **7**, 1425–1427 (1965)]
20. Komet Y., Low W., Linares R.C.: Phys. Lett. **19**, 473–474 (1965)
21. Kirton J.: Phys. Rev. **139**, A1930–A1933 (1965)
22. Voron'ko Yu.K., Zverev G.M., Meshkov B.B., Smirnov A.I.: Sov. Phys. Solid State **6**, 2225–2232 (1965) [Fiz. Tverd. Tela **6**, 2799–2808 (1965)]
23. Larson G.H., Jeffries C.D.: Phys. Rev. **141**, 461–478 (1966)
24. Mangum B.W., Hudson R.P.: J. Chem. Phys. **44**, 704–713 (1966)
25. Rector C.W., Pandey B.C., Moos H.W.: J. Chem. Phys. **45**, 171–179 (1966)
26. Watts R.K.: Solid State Commun. **4**, 549–552 (1966)
27. Antipin A.A., Kurkin I.N., Livanova L.D., Potvorova L.Z., Shekun L.Ya.: Sov. Phys. Solid State **8**, 2130–2132 (1967) [Fiz. Tverd. Tela **8**, 2664–2667 (1966)]
28. Bobrovnikov Yu.A., Zverev G.M., Smirnov A.I.: Sov. Phys. Solid State **8**, 1750–1756 (1967) [Fiz. Tverd. Tela **8**, 2205–2212 (1966)]
29. Bobrovnikov Yu.A., Zverev G.M., Smirnov A.I.: Sov. Phys. Solid State **9**, 1403–1409 (1967) [Fiz. Tverd. Tela **9**, 1794–1801 (1967)]
30. Kingsley J.D., Aven M.: Phys. Rev. **155**, 235–246 (1967)
31. Antipin A.A., Katyshev A.N., Kurkin I.N., Shekun L.Ya.: Sov. Phys. Solid State **10**, 468–474 (1968) [Fiz. Tverd. Tela **10**, 595–604 (1968)]
32. Mims W.B.: Phys. Rev. **168**, 370–389 (1968)
33. Watts R.K., Holton W.C.: Phys. Rev. **173**, 417–426 (1968)
34. Zverev G.M., Makarenko L.V., Smirnov A.I.: Sov. Phys. Solid State **9**, 2883–2884 (1968) [Fiz. Tverd. Tela **9**, 3651–3653 (1967)]
35. Brown M.R., Roots K.G., Williams J.M., Shand W.A., Groter C., Kay H.F.: J. Chem. Phys. **50**, 891–899 (1969)
36. Crowder B.L., Title R.S., Petit G.D.: Phys. Rev. **181**, 567–573 (1969)
37. Vasil'ev I.V., Zverev G.M., Makarenko L.V., Potkin L.I., Smirnov A.I.: Sov. Phys. Solid State **11**, 625–627 (1969) [Fiz. Tverd. Tela **11**, 776–779 (1969)]
38. Kurkin I.N., Tsvetkov E.A.: Sov. Phys. Solid State **11**, 3027–3029 (1970) [Fiz. Tverd. Tela **11**, 3610–3613 (1969)]
39. Abraham M.M., Finch C.B., Kolopus J.L., Lewis J.T.: Phys. Rev. B **3**, 2855–2864 (1971)
40. Sattler J.P., Nemarich J.: Phys. Rev. B **4**, 1–5 (1971)
41. Kornienko L.S., Rybaltovskii A.O.: Sov. Phys. Solid State **15**, 1322–1326 (1974) [Fiz. Tverd. Tela **15**, 1975–1983 (1973)]
42. Newman R.C., Woodward R.J.: J. Phys. C: Solid State Phys. **7**, L432–L435 (1974)
43. Antipin A.A., Klimachev A.F., Korableva S.L., Livanova L.D., Fedii A.A.: Sov. Phys. Solid State **17**, 664–668 (1975) [Fiz. Tverd. Tela **17**, 1042–1049 (1975)]
44. Kulpa S.M.: J. Phys. Chem. Solids **36**, 1317–1321 (1975)
45. Antipin A.A., Livanova L.D., Fedii A.A.: Sov. Phys. Solid State **20**, 1030–1034 (1978) [Fiz. Tverd. Tela **20**, 1783–1789 (1978)]
46. Korableva S.L.: Sov. Phys. Solid State **20**, 2139–2140 (1978) [Fiz. Tverd. Tela **20**, 3701–3703 (1978)]
47. Edgar A., Jones G.D., Presland M.R.: J. Phys. C: Solid State Phys. **12**, 1569–1585 (1979)
48. Baeumler M., Schneider J., Köhl F., Tomzig E.: J. Phys. C **20**, L963–L965 (1987)
49. Masterov V.F., Shtel'makh K.F., Zakharenkov L.F.: Sov. Phys. Semicond. **21**, 223 (1987) [Fiz. Tekh. Poluprovodn. **21**, 365–366 (1987)]
50. Boyn R.: Phys. Status Solidi B **148**, 11–47 (1988)
51. Grachev V.G., Zaripov M.M., Ibragimov I.R., Rodionova M.P., Falin M.L.: Sov. Phys. Solid State **31**, 82–84 (1989) [Fiz. Tverd. Tela **31**, 149–153 (1989)]
52. Klein P.B., Moore F.G., Dietrich H.B.: Appl. Phys. Lett. **58**, 502–504 (1991)
53. Masterov V.F.: Sov. Phys. Semicond. **27**, 791–801 (1993) [Fiz. Tekh. Poluprovodn. **27**, 1435–1452 (1993)]
54. Dziesiaty J., Müller St., Boyn R., Buhrow Th., Klimakow A., Kreissl J.: J. Phys. Condens. Matter **7**, 4271–4282 (1995)

55. Milori D.M.B.P., Moraes I.J., Hernandes A.C., de Souza R.R., Siu Li M., Terrile M.C., Barberis G.E.: Phys. Rev. B **51**, 3206–3209 (1995)
56. Priolo F., Franzò G., Coffa S., Polman A., Libertino S., Barklie R., Carey D.: J. Appl. Phys. **78**, 3874–3882 (1995)
57. Carey J.D., Donegan J.F., Barklie R.C., Priolo F., Franzò G., Coffa S.: Appl. Phys. Lett. **69**, 3854–3856 (1996)
58. Ishiyama T., Katayama E., Murakami K., Takahei K., Taguchi A.: J. Appl. Phys. **84**, 6782–6787 (1998)
59. Strnisa F.V., Corbett J.W.: Cryst. Lattice Defects **5**, 261–268 (1974)
60. Stevens K.W.H.: Proc. Phys. Soc. Lond. A **65**, 209–215 (1952)
61. Lea K.R., Leask M.J.M., Wolf W.P.: J. Phys. Chem. Solids **23**, 1381–1405 (1962)
62. Abragam A., Bleaney B.: Electron Paramagnetic Resonance of Transition Ions. Oxford: Clarendon Press 1970.
63. Lewis H.R., Sabisky E.S.: Phys. Rev. **130**, 1370–1373 (1963)
64. Ham F.S., Ludwig G.W., Watkins G.D., Woodbury H.H.: Phys. Rev. Lett. **5**, 468–470 (1960)
65. Neubrand H.: Phys. Status Solidi B **86**, 269–275 (1978)
66. Falin M.L., Latypov V.A., Kazakov B.N., Leushin A.M., Bill H., Lovy D.: Phys. Rev. B **61**, 9441–9448 (2000)
67. Svare I., Seidel G. in: Paramagnetic Resonance (Low W., ed.), pp. 430–438. New York: Academic Press 1963.

Authors' address: Cornelis A. J. Ammerlaan, Van der Waals-Zeeman Institute, University of Amsterdam, Valckenierstraat 65, 1018 XE Amsterdam, The Netherlands